Chemical Geology 652 (2024) 122023

Contents lists available at ScienceDirect

Chemical Geology

journal homepage: www.elsevier.com/locate/chemgeo

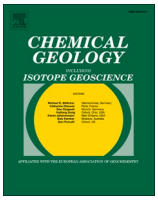

Short chain tricyclic terpanes as organic proxies for paleo-depositional conditions

Hong Xiao [a,*], Meijun Li [a], Benjamin J. Nettersheim [b]

[a] National Key Laboratory of Petroleum Resources and Engineering, College of Geosciences, China University of Petroleum, Beijing 102249, China
[b] MARUM – Center for Marine Environmental Sciences and Faculty of Geosciences, University of Bremen, 28359 Bremen, Germany

ARTICLE INFO

Editor: Hailiang Dong

Keywords:
Tricyclic terpanes
Depositional environments
Biological origin
Paleo-ecological reconstructions
Source rocks
Petroleum exploration

ABSTRACT

Reconstructing the paleo-environmental conditions that prevailed during the deposition of sediments provides invaluable information for paleo-ecological and evolutionary reconstructions and petroleum exploration. However, reconstructions of depositional environments based on sedimentary structures are often ambiguous, in particular if only core or mud chip samples are available. Organic proxies provide another avenue for paleo-depositional reconstruction of sedimentary rocks and related crude oils, but there is only a limited number of proxies and these rarely allow for unambiguous interpretations. Although tricyclic terpanes are among the most widely used depositional proxies, few studies calibrated terpane proxies with a large variety of samples. Here we show based on analyses of 485 oil and sediment samples from a variety of formations with well characterized depositional environments spanning in age from the late Paleozoic to Neogene, that the distribution of $C_{19} + C_{20}$, C_{21} and C_{23} tricyclic terpanes in ternary diagram has high predictive power to differentiate between marine/saline lacustrine, freshwater lacustrine, swamp and fluvial/deltaic depositional environments. Our analyses indicate that the tricyclic terpanes related parameters are not adulterated by even severe biodegradation or thermal maturation processes throughout the whole oil window, and our analyses of the largest terpane compilation to date encompassing >700 samples indicate robust proxy potential in post-Ordovician settings around the globe. This facile and widely applicable method for ecosystem definition can enhance a variety of petroleum, sedimentary and paleo-ecological studies and should best be used in concert with other organic and inorganic proxies for a detailed reconstruction of paleo-ecological conditions.

1. Introduction

The reconstruction of the depositional environment of a sedimentary rocks or related crude-oils is invaluable for paleo-ecological interpretations, reconstructions of sedimentary basins and petroleum exploration efforts. However, the interpretations of sedimentary features and proxy signatures are often ambiguous, resulting in a large degree of uncertainty in many paleo-depositional reconstructions. In particular, it is challenging to differentiate if water-laid facies were deposited in marine or non-marine environments. It is even more challenging to determine paleo-ecological conditions prevailing during the deposition of source rocks purely based on the chemical composition of crude oils that migrated into (possibly very distant) reservoirs - even more so if potential source rock facies are unknown or inaccessible for detailed sedimentary analyses. To predict migration pathways and determine probable sources of crude oils in order to improve exploration efforts, the nature and characteristics of the source rock often have to be deduced from the organic geochemical signatures of available oil samples. Molecular fossils or biomarkers, the geological transformation products of biomolecules that retain ecological information, can record information on the depositional environment in a similar manner to physical remains or fossils of organisms (Peters et al., 2005). Tricyclic terpanes (TT) have long been recognized to be ubiquitously distributed in sediments and petroleum of various origins and ages (Aquino Neto et al., 1982; Moldowan et al., 1983; De Grande et al., 1993; Cheng et al., 2016; Philp et al., 2021) and are well known to have high predictive power for source rock determinations (Zumberge, 1987). In the geological record, tricyclic terpanes in the carbon range of C_{20}–C_{25} were first detected simultaneously in the bitumen of Green River Formation oil shales (Anders and Robinson, 1971). Subsequently, an extended series of tricyclic terpanes with carbon numbers extending to at least C_{45} were recognized by metastable scanning gas chromatography–mass

* Corresponding author.
E-mail address: xiaohong@cup.edu.cn (H. Xiao).

https://doi.org/10.1016/j.chemgeo.2024.122023
Received 23 October 2023; Received in revised form 27 February 2024; Accepted 2 March 2024
Available online 7 March 2024

spectrometry (GC–MS) on the basis of a tricyclic terpane concentration prepared on an aluminum oxide column (Moldowan et al., 1983). The structures of C_{19} and C_{20} homologs of the tricyclic terpanes were proven by comparison with synthetic standards (Aquino Neto et al., 1982; Aquino Neto et al., 1986), containing a methyl substituent at C-13 and a regular isoprenoid side-chain at C-14 (Ekweozor and Strausz, 1982), as evidenced by the essential absence of C_{22} and C_{27}, and the occurrence of diastereomeric doublet peaks above C_{24} (Aquino Neto et al., 1982). Ten years later, De Grande et al. (1993) further reported tricyclic terpane series ranging from C_{19} to as high as C_{54} homolog in early to late Cretaceous rock extracts and oils from Brazil marginal basins (De Grande et al., 1993). Because the homologs of this series above C_{29} typically co-eluted with or are obscured by relative higher abundances of pentacyclic terpanes, tricyclic terpane analysis is often restricted to C_{19}–C_{29} homologs.

Although multiple potential precursors for the tricyclic terpanes have been proposed, no clear precursor/product relationship has been established. Generally, polyprenol (i.e., tricyclohexaprenol) membrane constituent of bacteria is widely accepted as one biological source of C_{19}–C_{29} tricyclic terpanes (Aquino Neto et al., 1982; Ekweozor and Strausz, 1982; Ourisson et al., 1982; Aquino Neto et al., 1983). From structural considerations, the 13-methyl, 14-alkylpodocarpane hydrocarbon skeleton was considered to be a cyclisation product of the regular polypropenols in membranes of bacteria (Ourisson et al., 1982) and/or archaea (Aquino Neto et al., 1982). In addition to prokaryotes, higher plant contributions were also suggested as potential sources of 13-methyl, 14-alkylpodocarpanes (Peters and Moldowan, 1993). Considering that tricyclic terpanes were identified as the major biomarkers in oil shales (~29% total organic carbon) of Permian age from Tasmania (Australia) known as tasmanite that are composed of silt, ash and compressed disks of fossil *tasmanites* or tasmanitids considered to be fossil green algal remains such as zoosporangia of prasinophyte algae (Simoneit et al., 1990), algae are also considered likely sources of tricyclic terpanes (Azevedo et al., 1992; Simoneit et al., 1993; Revill et al., 1994).

Recently, the discrimination diagrams of $C_{19} + C_{20}/C_{23}TT$ vs. $C_{23}/C_{21}TT$ (Tao et al., 2015) and $C_{23}/C_{21}TT$ vs. $C_{21}/C_{20}TT$ (Wang et al., 2023) have been used to provide reliable and detailed environmental information, but it cannot always distinguish the freshwater lacustrine oils from saline lacustrine oils (Tao et al., 2015). Xiao et al. (2019a, 2019b, 2019c) then preliminarily established a ternary diagram of the relative abundance of C_{19}–$C_{23}TT$ to distinguish the different depositional environments. In addition, Philp et al. (2021) found that both crude oils and source rocks from the Anadarko Basin show uncommon terpane distribution patterns with dominated fingerprints of tricyclic terpanes and the virtual absence of hopanes, which was explained as thermal maturity being the most significant driving force. Here, we determined C_{19}–C_{23} tricyclic terpanes signatures of 485 sediments and oil samples and compared depositional signatures to extensive literature compilations, to assemble the largest tricyclic terpanes compilation to date, comprising >700 samples reflecting various depositional environments. With this dataset, we test the predictive power of these biomarkers for the reconstruction of depositional environments and discuss biosynthetic pathways, and geological processes affecting triterpane signatures in sedimentary rocks and crude oils.

2. Samples and experimental method

2.1. Samples

We determined C_{19} to C_{23} TT signatures for 485 sediment and crude oil samples from various geographical locations, including dozens of basins in the north, south, east, northeast and northwest of China, and several basins in Africa, spanning an age range from the late Paleozoic to Neogene. This large sample compilation comprehensively represents various depositional environments ranging from marine, freshwater lacustrine, saline lacustrine to terrigenous settings.

For validating the use of ternary diagram for the identification of depositional settings we further incorporate previously published triterpene data from samples of known provenance, encompassing 144 oil samples generated from marine, lacustrine and paralic/deltaic source rocks reported by Zumberge (1987), 25 source rocks reported to derive from Ordos freshwater lacustrine depositional setting by Pan et al. (2017), 19 oil samples generated from freshwater lacustrine source rocks reported by Xiao et al. (2019a), 32 oil samples generated from freshwater lacustrine, saline lacustrine, marine and terrigenous facies source rocks reported Tao et al. (2015).

2.2. Experimental methods

Experimental procedures and methods employed for our tricyclic terpanes analysis conducted in the National Key Laboratory of Petroleum Resources and Engineering, China University of Petroleum (Beijing), comprise extraction of soluble organic matter, wet chemical separation of extracts and oils into four fractions, and GC–MS analysis of the saturate hydrocarbon fractions.

The soluble organic matters were extracted from powder samples (~100 g) with 300 ml of dichloromethane by Soxhlet apparatus for 72 h, and the extract mixtures were concentrated using a rotary evaporator. Then the extracts and crude oils were dissolved with 40–50 ml petroleum ether in glass container, and slowly poured the solutions into a funnel stuffed with cotton to remove insoluble asphaltenes. The residual solution was further separated into saturate, aromatic, and resin fractions through a chromatography column sequentially filled with 3 g of silica gel and 2 g of alumina, using 30 ml of petroleum ether (5 ml each time), 20 ml of mixture of dichloromethane and petroleum ether (2:1, *v*/v) (5 ml each time), and 20 ml mixture of dichloromethane and methanol (93:7, v/v) as eluents, respectively.

Saturate fraction was analyzed by gas chromatography–mass spectrometry (GC–MS) to determine C_{19}–C_{23} tricyclic terpanes signatures. The analytical instrument of GC–MS is composed of an Agilent 6890 gas chromatograph and Agilent 5975i mass spectrometer. The oven temperature was initially set at 50 °C and kept for 1 min, then programmed to 120 °C at 20 °C/min, finally to 310 °C at 3 °C/min and kept for 25 min. The HP-5 MS fused silica capillary column (30 m × 0.25 mm internal diameter, with 0.25 μm film) was equipped in GC instrument, and the injection volume is 1.0 μl. The Helium was used as carries gas at 1.0 ml/min constant flow. The MS source was operated in electron impact with ionization energy of 70 eV and a scanning range of 50–600 Da.

3. Results

C_{19}–C_{29} tricyclic terpanes can usually be readily recognized in GC–MS *m/z* 191 selected ion chromatograms. They are present in virtually all biomarker-bearing geological samples encompassing a large variety of biological sources, depositional conditions and thermal maturities. In the following, we elucidate the C_{19}–C_{23} tricyclic terpanes distribution patterns in different types of depositional environments. To illustrate differences in our facies groups, we show representative chromatograms for each type of depositional environment (Fig. 1). As boxplot analyses allow to intuitively grasp fundamental characteristics of data groups, we further summarized the relative abundances of $C_{19} + C_{20}$, C_{21} and C_{23} tricyclic terpanes for each data subset reflecting a particular type of depositional in a box plot. The composite figure allows to readily visualize the main differences in TT distributions between the five different types of depositional environments (Fig. 1). The relative abundance of $C_{19} + C_{20}$, C_{21} and $C_{23}TT$ are the percentage of peak areas of $C_{19} + C_{20}$, C_{21} and $C_{23}TT$ to the total peak areas of C_{19}-$C_{23}TT$, respectively.

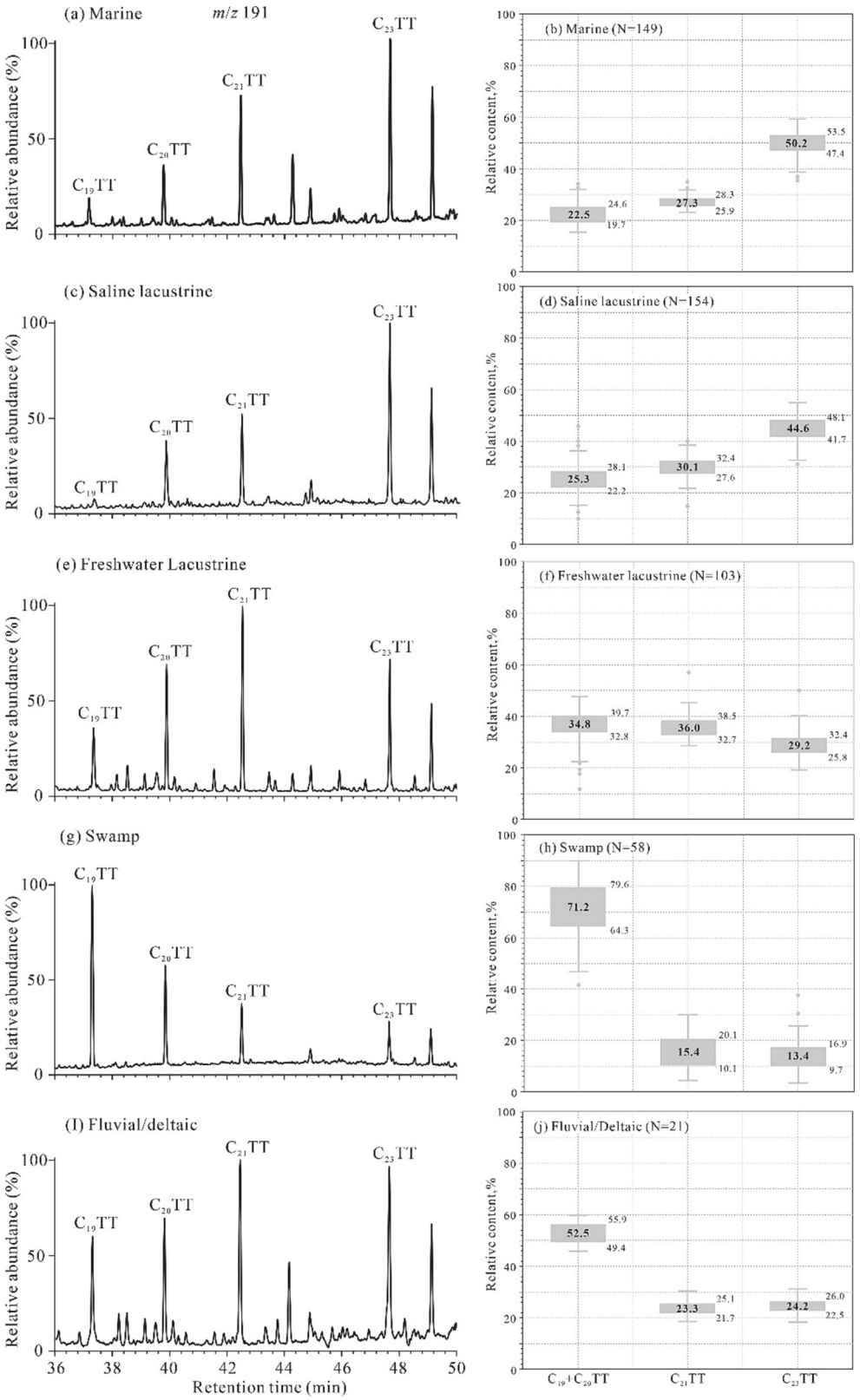

Fig. 1. C_{19}-C_{23} TT distribution in *m/z* 191 mass chromatogram and boxplot of percentages of C_{19+C20}TT, C_{21}TT, and C_{23}TT in samples from various sedimentary facies. Notes: 'TT' is the abbreviation for tricyclic terpane; the bold numbers in the box represent the average value; 'N' represents the quantity of samples.

3.1. Marine sedimentary setting

Our analysis comprises 149 marine sediments and related crude oils from different locations and geological ages (Table S1), including the Permian Zhesi Formation marine mudstones in the Songliao Basin (NE China) (Ming et al., 2015), and the Cretaceous marine shales and related crude oils from the Termit Basin (Niger) (Xiao et al., 2019c). A typical distribution of C_{19}–C_{23} tricyclic terpanes in *m/z* 191 mass

chromatograms in marine sediments is illustrated in Fig. 1a from the Termit Basin, Niger. The C_{23} tricyclic terpane is typically the dominant homolog among C_{19}–C_{23} tricyclic terpanes with a 'rising' distribution pattern from C_{19} to C_{23} and low abundances of the C_{22} homolog reflecting the point of isoprenoidal branching (methylation) of the side-chain. A boxplot analysis of the relative abundances of C_{19} + C_{20}, C_{21} and C_{23} terpanes for the 149 marine samples in our data set highlights the strong dominance of the C_{23} tricyclic terpane homolog in marine samples, with C_{23} TT abundances mainly ranging from 47.4%–53.5% for most samples (Fig. 1b), with a maximum value in our data set of 59.4% (Table S1). The relative percentages of C_{19} + C_{20} and C_{21} TTs are both <30.0%, but the average percentage of C_{21} TT (27.3%) is slightly higher than that of C_{19} + C_{20} TTs (22.5%), which are mainly in the value ranges of 19.7%–24.6% and 25.9%–28.3%, respectively (Fig. 1b).

3.2. Saline water lacustrine sedimentary setting

In addition, we compiled TT distributions for facies previously identified to reflect saline lacustrine depositional conditions, comprising 154 samples from the Qaidam Basin (Zhu et al., 2005; Zhang et al., 2011; Zhang et al., 2018), the Bohai Bay Basin (i.e., Dongpu and Dongying depressions) (Li et al., 2003; You et al., 2021), and the Mahu Depression of the Junggar Basin (Wang et al., 2019; Chen et al., 2022) (Table S2). Interestingly, the distribution pattern of C_{19}–C_{23} tricyclic terpanes and the relative percentages of C_{19} + C_{20}, C_{21} and C_{23} tricyclic terpanes of the saline lacustrine samples are indistinguishable from the marine samples in our dataset, exhibiting the 'rising' distribution pattern from C_{19} to C_{23} tricyclic terpanes and C_{23} tricyclic terpane as the dominant homolog (Fig. 1c) with the relative percentage mainly ranging from 41.7% to 48.1% and average value of 44.6% (Fig. 1d). Overall, above features are in agreement with previous evidence for oils and sediments from saline lacustrine environment in China, Brazilian and the Green River Formation (Powell, 1986; Mello et al., 1988; Tao et al., 2015). De Grande et al. (1993) noted that the biological sources of TTs could be affected by the salinity of the depositional environment, resulting the inferences of a salinity influence on tricyclic terpanes distributions with precursor organisms of tricyclic terpane series (up to C_{54}) thought to proliferate under moderate salinity (saline lacustrine to marine carbonate) depositional conditions (De Grande et al., 1993). Although the specific precursors for the tricyclic terpanes are not yet known, the strong similarity between marine and saline lacustrine depositional environments in our dataset supports the inference that the precursor organisms of longer tricyclic terpanes (in our case C_{23}) are indeed more prosperous in the saline water conditions. This observation further points towards a direct biological control on TT distributions with particular dominant source organisms for shorter and longer tricyclic terpane homologs.

3.3. Freshwater lacustrine sedimentary setting

A total of 103 sediment and crude oil samples were collected from freshwater lacustrine facies (Table S3), including the Eocene Shahejie Formation sediments from the Liaohe Basin (NE China) (Hu et al., 2005; Xiao et al., 2018), the Triassic lacustrine oils from the Tabei Uplift and the Paleogene lacustrine oils from the Kuqa Depression in the Tarim Basin (NW China) (Zhang and Huang, 2005; Yang et al., 2016), as well as the Cretaceous lacustrine sediments and related oils from the Bonger Basin (Chad) and Muglad (Sudan) (Table S3) (Genik, 1993; Xiao et al., 2021a). In general, freshwater lacustrine samples are dominated by C_{21} tricyclic terpane among C_{19}–C_{23} homologs (Fig. 1e). The relative percentage of C_{21} tricyclic terpane is mainly in the range of 32.7%–38.5% (Fig. 1f) with an average of 36.0% and maximum value up to 57.5% (Table S3), which is consistent with previous reports (Zumberge, 1987; Tao et al., 2015). The sum of relative abundance of C_{19} and C_{20} tricyclic terpanes is similar to that of C_{21} tricyclic terpane, with an average value of 34.8% (Table S3). The abundance of C_{23} tricyclic terpane is slightly lower than that of C_{19} + C_{20} and C_{21} tricyclic terpanes, with the main range of 25.8%–32.4% (Fig. 1f).

3.4. Swamp sedimentary setting

Our swamp facies subset comprises 3 Jurassic coal samples from the Tabei Uplift in the Tarim Basin (NW China) (Sun et al., 2003; Zhang and Huang, 2005), 12 Carboniferous-Permian coal samples from the north China (Luo et al., 2005), 23 Paleogene coal measure source rocks and related oils from the Xihu Sag in the East China Sea Shelf Basin (Cheng et al., 2020), 16 Paleogene coal measure source rocks from Baiyun Depression (Xiao et al., 2018; Fu et al., 2019), as well as 4 coal-derived oil samples from the Niudong area in the Qaidam Basin (Zhou et al., 2016) (Table S4). The C_{19}–C_{23} tricyclic terpanes in these samples have a consistent distribution, showing a strong dominance of low-carbon number tricyclic terpanes (C_{19}–C_{20}) with a 'declining' distribution pattern from C_{19} to C_{23} tricyclic terpanes (Fig. 1g). The relative percentage of C_{19} + C_{20} tricyclic terpanes is >60.0%. Relative C_{19} + C_{20} tricyclic terpanes abundances are particularly high in the Carboniferous-Permian coal samples from north China, ranging from 70.0%–90.0% with an average of 81.0% (Table S4). For our rock or related oil samples, the relative abundances of C_{21}TT and C_{23}TT are almost <20.0% and mainly in the range of 10.1%–20.1% and 9.7%–16.9%, respectively (Fig. 1h).

3.5. Fluvial /deltaic sedimentary setting

The Paleogene Eocene Liushagang Formation sediments in the Beibuwan Basin (South China Sea) and related oils were previously inferred to have been deposited under fluvial/deltaic depositional conditions (Table S5) (Gan et al., 2020; Zeng et al., 2022). They display high pristane/phytane ratio (>2.0) characteristic for terrigenous (transported) organic matter and substantial amounts of the higher plant marker compound oleanane (oleanane/C_{30}hopane > 0.25) indicative of substantial terrigenous organic matter contributions (Huang et al., 2011; Xiao et al., 2018).

In the boxplot and representative mass chromatogram *m/z* 191, it can be seen that the relative abundance of short-chain compounds (C_{19} and C_{20} tricyclic terpanes) in the fluvial/deltaic samples is not as high as in the swamp samples, but higher than in the other facies (Fig. 1i-j). The sum of the relative abundances of short-chain compounds (C_{19} + C_{20} tricyclic terpanes) mostly ranges from 49.4%–55.9% with an average value of 52.5%. The relative abundance of C_{19} + C_{20} tricyclic terpanes in the fluvial/deltaic samples is between the typical values of freshwater lacustrine and swamp facies: generally higher than that of freshwater lacustrine facies and lower than swamp facies samples. The boxplots show that there is very little overlap in C_{19} + C_{20} TT abundances in swamp versus fluvial deltaic and freshwater lacustrine samples, while the marine and saline lacustrine samples are clearly distinguished by elevated abundances of C_{23}TT.

4. Discussion

For the application of organic proxies, it is necessary to determine the effects of maturity and biodegradation on target molecular properties (Mello et al., 1988; Peters et al., 2005). In this study, we consider the variations of the relative contents of C_{19} + C_{20}TT, C_{21}TT, C_{23}TT and related parameters with increasing maturity and biodegradation intensity.

4.1. Thermal maturity influence

Tricyclic terpanes are known to be more stable against geothermal degradation than pentacyclic hopanes and tricyclic/pentacyclic terpane ratios can therefore act as source as well as maturity parameter (Seifert and Moldowan, 1978; Aquino Neto et al., 1983). Many studies have

reported that the abundance of the tricyclic terpanes relative to 17a(H)-hopanes will progressively increase with increasing thermal maturity (e.g., tricyclic terpanes/(tricyclic terpanes + hopanes) ratio) (Seifert and Moldowan, 1978; Graas, 1990; Peters et al., 2005), which was attributed by some workers to a preferential release of the tricyclics from the kerogen at higher levels of maturity (Aquino Neto et al., 1983). Farrimond et al. (1999) further noted that in the rock samples subjected to geologically rapid heating by an igneous body, TT maturity proxies (e.g., tricyclic terpanes/ (tricyclic terpanes + hopanes) ratio) also show a significant increase. As shown in the Fig. 2a, we determined tricyclic terpane parameters for 17 rock samples spanning a depth from 2826 to 4733 m, corresponding to vitrinite reflectance value (%Ro) range from 0.58% to 1.47% (Table S6) and thus covering a maturity range throughout the whole oil window (i.e., early to late stage of oil generation) in the S202 well from the Liaohe Sub-basin (North China). As expected from the higher thermal stability of tricyclic terpanes compared to hopanes (Peters et al., 2005), the ratio of C_{19}–C_{23}TT to C_{27}–C_{35} 17a(H)-hopanes (TT/H) gradually increases with the increase of burial depth and thermal maturity below a depth of 3.5 km corresponding to Ro of 0.63% (Fig. 2a and Table S6). However, very few studies have investigated a potential maturity effect on the distribution patterns of short chain tricyclic terpane homologs (C_{19}–C_{23}TT). A strong correlation between burial depth and TT/H ratio in the main oil window depth range between 3.5 and 4.8 km reveals thermal maturity as the main control on the TT/H ratio in the main oil window (Fig. 2a), while substantial deviations from the general depth trend point towards inheritance of a source influence that is not completely overprinted by the thermal maturity influence. Our analysis further shows that the C_{21}/C_{20}TT and C_{21}/C_{23}TT ratios and the relative abundances of C_{19} + C_{20}TT, C_{21}TT, and C_{23}TT maintain a relatively stable distribution throughout the burial range. Except for slight irregular fluctuations, the parameter values have no correlation with the increase of burial depth and %Ro (Fig. 2b-f), revealing a similar thermal stability for the different (C_{19}–C_{23}) tricyclic terpane homologs throughout the oil window or their similar thermogenic mechanisms transformed from the precursors. Previous hydropyrolysis experiments also showed that within a pyrolysis temperature range between 310 °C to 500 °C (Wang et al., 2012; Chen et al., 2017), the absolute abundance of C_{19}–C_{23} tricyclic terpanes and TT/H ratio increases, but the TT distribution pattern does not change significantly. Therefore, we propose that proxies based on TT homolog distributions are effective indicators for identification of biological sources and depositional environments for high-maturity organic matter at least until the end of the oil window.

4.2. Biodegradation influence

The Muglad Basin in Sudan is one of the Mesozoic-Cenozoic passive rift basins in the Central African Shear Zone (McHargue et al., 1992; Xiao et al., 2019a). The Muglad Basin oil samples analyzed in the study belong to the same oil family, which originate from the source rocks of the Cretaceous Abu Gabra Formation mudstones (Xiao et al., 2019a). Yang et al. (2019) have proposed that these crude oils have suffered different degrees of biodegradation. To determine the likely effects of biodegradation on TT parameters, in this study we compare the distribution patterns of C_{19}–C_{23}TT in the non-biodegraded (e.g., wells HBC-1, MG 33–1 and MG 18–2), slightly biodegraded (e.g., wells HBE-1, MG-21 and MG-17), moderately biodegraded (e.g., wells MG 10–3, KY-5 and MG-9), and heavily biodegraded oils (e.g., wells MG 1–7, MG-20 and MG-26 with exhibiting a substantial 25-norhopane-enrichment) (Yang et al., 2019).

According to previous studies, tricyclic terpanes generally show a strong resistance to biodegradation, and can still be preserved when regular hopanes have been quantitatively depleted (Seifert and Moldowan, 1978; Cheng et al., 2016). For example, in severely biodegraded oils, the *m/z* 191 mass chromatogram is often dominated by tricyclic terpanes with only trace amounts of hopanes (Peters et al., 2005). Fig. 3 shows that in representative crude oils from the Muglad Basin that exhibit different degrees of biodegradation, the C_{19}–C_{23}TT distribution patterns remain very similar (Fig. 3 and Table S7). As is known to all, the Cretaceous McMurray oil sands in the Alberta Basin (Canada) are the result of microbial modification (Head et al., 2003). However, C_{19}-C_{23}TT distributions were shown to remain unaltered in these heavily biodegraded oil sands with the C_{23}TT as the main peak (Table S8), which is consistent with the understanding of hydrocarbon supply from marine source rocks (Bennett and Jiang, 2021). Our analyses thus indicate that C_{19}–C_{23}TT distributions are unlikely to be substantially affect by biodegradation processes. Thus, we conclude that proxies based on the relative distribution of TT can be effectively used to evaluate biological

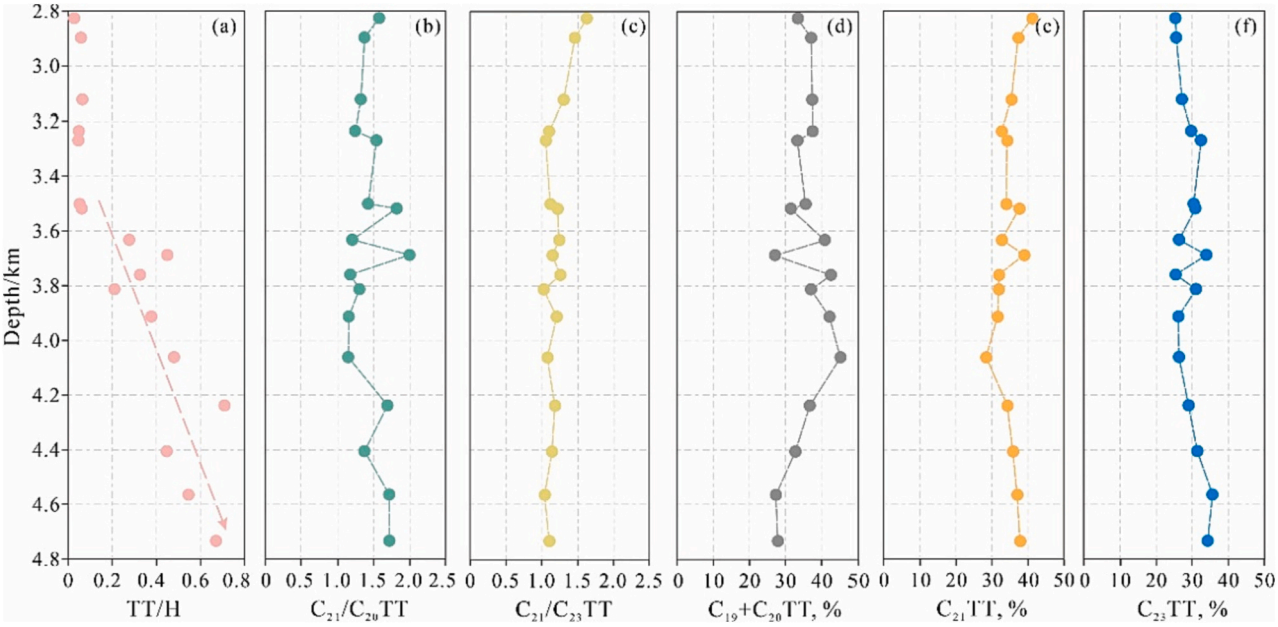

Fig. 2. Depth trends of tricyclic terpane parameters of crude oils in well S202, Liaohe Basin (China). a) Ratio of the sum of C_{19} to C_{23} TT to C_{27}–C_{35} 17a(H)-hopanes (TT/H); b) Ratio of C_{21}TT/C_{20}TT and c) C_{21}TT/ C_{23}TT; d) Relative abundance of C_{19} + C_{20}TT and e) C_{21}TT and f) C_{23}TT.

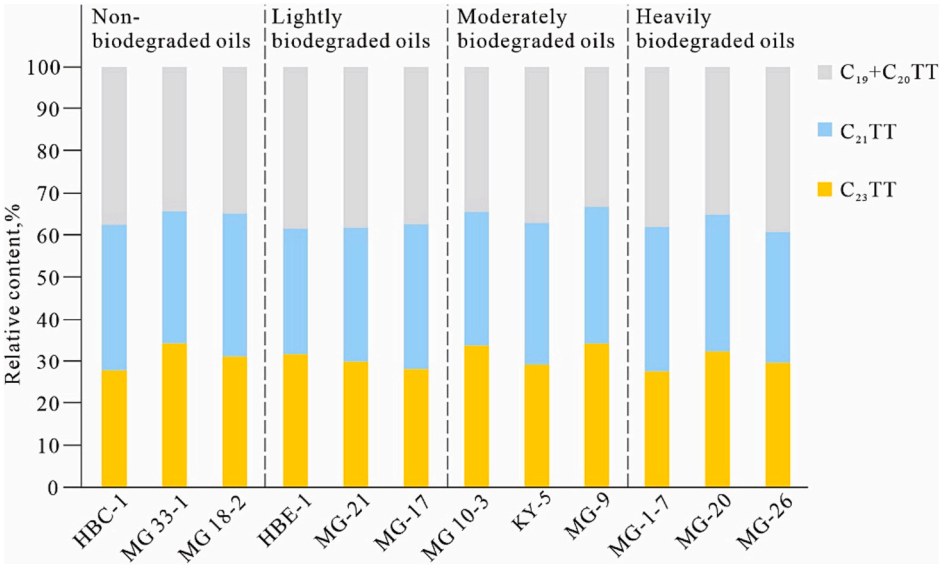

Fig. 3. Percentage of C_{19} + C_{20}TT, C_{21}TT, C_{23}TT in the crude oils with different degrees of biodegradation from the Muglad Basin, Africa.

sources and depositional environments in severely biodegraded oil, where other saturate biomarkers were strongly altered (Palacas et al., 1986; Stojanović et al., 2001).

4.3. Potential biological precursors

Unlike other common biomarker series, such as steroids and hopanoids, the functionalized precursors of tricyclic terpane series have not yet been definitively established. However, the tricyclic terpanes with different carbon numbers were selectively enriched in different sedimentary environments with different organic composition, pointing towards preferential formation of different TT homologs from particular biomolecules by distinctive source organisms with strong environmental preferences and/or by a variety of different source organisms that adjust TT precursor biomolecules depending on the prevailing environmental conditions.

Generally, hexaprenol [**1**], as a possible precursor of tricyclic terpanes (up to C_{30}), was widely proposed to be derived from membrane constituent of prokaryotic bacteria (Aquino Neto et al., 1982), archaea (Holzer et al., 1979; Aquino Neto et al., 1982), and now-extinct Tasmanites (Simoneit et al., 1990; Aquino Neto et al., 1992; Azevedo et al., 1992; Greenwood et al., 2000). According to the proposed biosynthetic reaction schemes for the formation of tricyclic terpanes (Fig. 4), hexaprenol [**1**] can biologically transformed into the intermediate product tricyclohexaprenol [**2**] by a cyclization reaction under anaerobical conditions (Aquino Neto et al., 1982), and then directly convert into the corresponding saturate tricyclic terpanes [**3**] through diagenetic hydrogenation reactions. The relative abundance of shorter or longer homologs during biological or diagenetic degradation may depend not only on depositional conditions (e.g., redox) such as preferential cleavage of the isoprenoid side-chains during prolonged aerobic degradation (Schwark and Frimmel, 2004), but also on the size (i.e.,

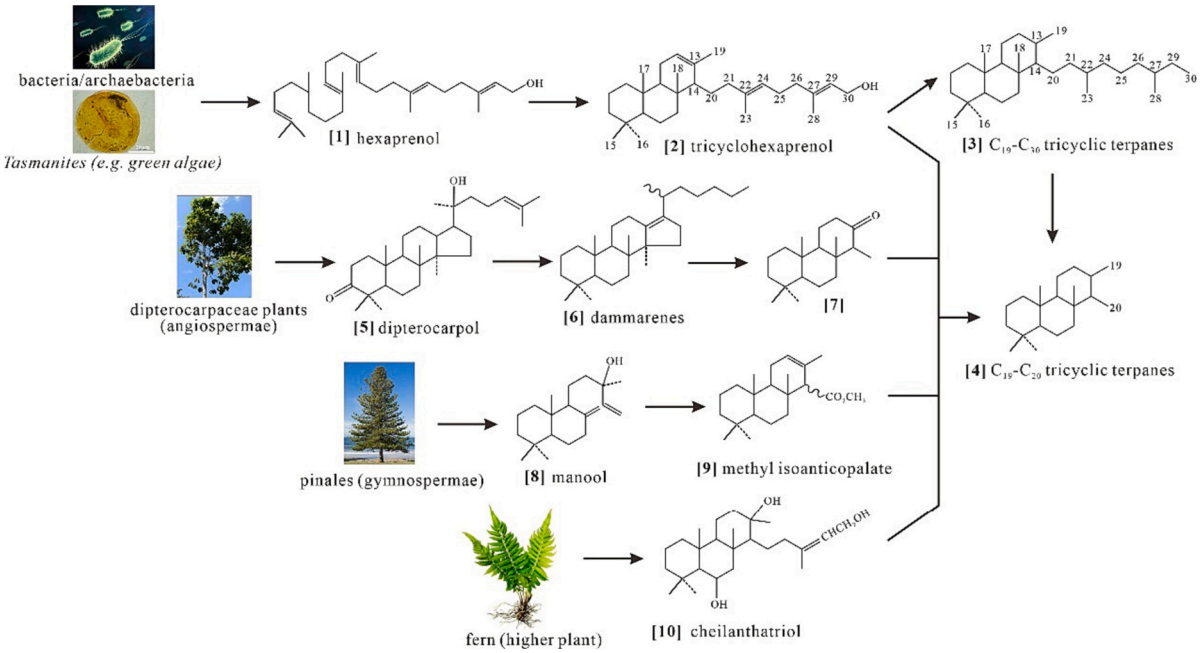

Fig. 4. Hydrocarbon structures and potential formation pathways of C_{19}-C_{23} tricyclic terpanes.

carbon number) and functionalization of different biological precursor molecules other than tricyclohexaprenol (Fig. 4).

In our data set, C_{23} tricyclic terpane is always prominent in marine and saline sediments and crude oils from saline lacustrine or marine sources (Fig. 1), and a large number of previous reports also revealed similar environmental affinities (Aquino Neto et al., 1983; Zhu et al., 2005; Tao et al., 2015; You et al., 2020). Thus, it is reasonable to propose that the dominant producers of C_{23} tricyclic terpane precursors, such as bacteria and certain algae, mainly flourish in saline water depositional conditions (e.g., marine and saline lacustrine). It is possible that under the depositional (e.g., redox) conditions prevailing under saline conditions, tricyclohexaprenol would be cleaved at the site of unsaturation located adjacent to the branching point of the side-chain (Fig. 4). If this was the dominant mechanisms for the formation of C_{23}TT, we would predict a similar relative enrichment of C_{28}TT, C_{33}TT, C_{38}TT, etc. in saline samples. Such an enrichment may be masked by a dominance of hopane signals in this elution range of most GC–MS (*m/z* 191 partial ion) chromatograms, but this may be tested through suitable MRM experiments with GC conditions that minimize co-elution and/or wet-chemical separation of tri- and pentacyclic fractions prior to GC–MS analyses. However, it is difficult to imagine how environmental conditions alone such as salinity may result in such stark differences of short-chain TT distributions between different depositional environments if tricyclohexaprenol was the main precursors in all environments. We therefore recognize the existence of other major precursors in at least some depositional environments. There are relatively few studies on the precursors of C_{21}TT that may have diverse biological sources. We observed the highest relative abundance of C_{21}TT in freshwater lacustrine sediments and crude oils (Fig. 1e), which is also consistent with the results of previous studies (Xiao et al., 2021a; Zumberge, 1987).

These observations thus point towards the preferential production of precursors to C_{21}TT in freshwater and precursors to C_{23}TT in saline environments (i.e., likely tricyclohexaprenol or other extended tricyclic triterpenoids) either by different types of organisms adapted to different salinities or by the same types of microorganisms in response to varying environmental conditions, maybe even as a direct or indirect response to osmotic stress.

According to the proposed biosynthetic reaction schemes for the formation of C_{19} and C_{20} tricyclic terpanes (Fig. 4), the side-chain lacking homologs are likely to not only derive from progressive degradation of extended (e.g., C_{21}–C_{30} or even longer tricyclic terpenoids), but also from additional biological sources. In particular, angiosperms (e.g., dipterocarpaceae), gymnosperms (e.g., pinales), and other high plant (e.g., fern) are considered likely biological sources of short C_{19} and C_{20} TT. As depicted in Fig. 4, the dipterocarpaceae angiosperms can produce large amounts of dipterocarpol [**5**] and related dammarenes [**6**], both of which can be converted into C_{19} and possibly C_{20} TT through oxidation, hydrogenation and other reactions. Other likely precursors of C_{19} and C_{20} TT are manool [**8**] produced by the gymnosperms pinales (Fig. 4) (Aquino Neto et al., 1982). For example, manool [**8**] was detected in hexane-extracts of the New Zealand pink pine *Halocarpus biforme* (Carman and Duffield, 1993). In addition, cheilanthatriol [**10**] that has been detected in petroleum ether extracts of ferns (e.g., *Cheilanthes farinosa* Kaulf.) (Fig. 4) (Khan et al., 1971), is another potential precursors of short-chain (up to C_{25}) tricyclic terpanes with the substantially shorter side-chain expected to result in higher relative abundances of short chain TT during degradation processes compared to the same degree of diagenetic degradation affecting tricyclohexaprenol or other extended tricyclic terpenoids. In our data set, sediments or related crude oils with substantial organic matter contributions from higher plants (i.e., swamp and fluvial/deltaic samples) show substantial enrichment of C_{19} and C_{20} tricyclic terpanes. Moreover, previous studies reported a dominance of C_{19} and C_{20} tricyclic terpanes in terrigenous samples, especially in coal samples and coal-derived oils (Peters and Moldowan, 1993; Hanson et al., 2000; Tao et al., 2015) and elevated abundances of C_{19}-C_{20} tricyclic terpanes are usually consistent with terrestrial organic matter contributions (Reed, 1977; Preston and Edwards, 2000; Volk et al., 2005).

Therefore, elevated abundances of C_{19} and C_{20} TT in Late Paleozoic and younger samples can be expected to be largely derived from higher plant sources and/or associated (e.g., soil) microbiota. Proxies encompassing C_{19} and C_{20} TT should thus be carefully considered (i.e., recalibrated) for samples that were deposited prior to the expansion of higher plants. However, higher plants are clearly not the only potential sources of substantial amounts of short-chain TT as some geological samples that were deposited prior to the evolution of land plants also show a predominance of C_{19} and C_{20} tricyclic terpanes, such as shales from the Mesoproterozoic Xiamaling Formation on the North China Craton (Xiao et al., 2021b) and crude oils generated from Ordovician source rocks (Zumberge, 1983). Some workers therefore deduced a contribution of specific bacteria and algae that are restricted to particular environmental conditions (Aquino Neto et al., 1983; Xiao et al., 2021b). Considering the likely diagenetic formation of C_{19} and C_{20} TT from dammarene precursors (Fig. 4), we hypothesize that putative microbial sources of dammarenes, that were inferred from the widespread occurrence of dammarenes in marine sediments and their carbon isotopic signatures (Meunier-Christmann et al., 1991), are likely sources of C_{19} and to a lesser degree C_{20} TT in aquatic settings that lack substantial higher plant input.

4.4. Ternary diagram for inferring depositional environments

4.4.1. Exploring tricyclic terpane distributions in our dataset

As shown in Fig. 5a, the relative percentages of C_{19} + C_{20}TT, C_{21}TT and C_{23}TT are used as the three end-members of the ternary diagram. The 485 samples from marine/saline lacustrine, freshwater lacustrine, swamp and fluvial/deltaic facies are discretely distributed in different areas (Fig. 5a, Table S1–5). The sediments and crude oils deposited in marine/saline lacustrine environments have similar distribution pattern of C_{19}–C_{23} tricyclic terpanes with a predominance of C_{23}TT. Freshwater lacustrine sediments and crude oils plot towards the center of the ternary diagram with a high relative abundance of C_{21}TT which may reflect enhanced production of C_{21}TT precursors compounds in freshwater environments. Fluvial/deltaic and swamp samples are shifted towards the bottom left corner of the ternary diagram with a dominance of C_{19} + C_{20}TT, with swamp samples showing the strongest enrichment of C_{19} + C_{20}TT (Fig. 5a).

Although many parameters of tricyclic terpanes (e.g., (C_{19} + C_{20})/C_{23}TT, (C_{19} + C_{20} + C_{21})/(C_{23} + C_{24})TT, C_{22}/C_{21}TT, C_{23}/C_{21}TT, C_{24}/C_{23}TT, C_{26}/C_{25}TT, ΣTT/ΣHop, and ETR) and cross plots of these parameters (e.g., C_{26}/C_{25}TT vs. C_{31}R/C_{30}H, C_{22}/C_{21}TT vs. C_{24}/C_{23}TT, (C_{19} + C_{20})/C_{23}TT vs. C_{23}/C_{21}TT, C_{23}/C_{26}TT, and (C_{19} + C_{20} + C_{21})/(C_{23} + C_{24})TT vs. ΣTT/ΣHop) (Farrimond et al., 1999; Peters et al., 2005; Tao et al., 2015; Xiao et al., 2019c) have been established and used to identify diverse lithology, depositional conditions, thermal maturity and biodegradation level, none of them have been widely applied in published paleo-ecological and petroleum system studies. The reasonable separation of different depositional environments in our ternary diagram (Fig. 5b) suggests that determination of short chain tricyclic terpane distributions in a ternary diagram is a simple, convenient, and powerful method for the determination of the paleo-depositional environments of sediment and crude-oil samples with a wide range of thermal maturity (Fig. 3) and biodegradation (Fig. 4).

4.4.2. A global compilation of tricyclic terpanes and the world-wide applicability of the ternary diagram for identifying paleo-depositional environments

To determine the validity and applicability of the ternary diagram of C_{19} + C_{20}TT, C_{21}TT and C_{23}TT established in our study, we added a large compilation of previously characterized samples. Zumberge (1987) predicted the depositional environments of five categories of sediments by biomarkers. Based on the tricyclic terpane data reported by

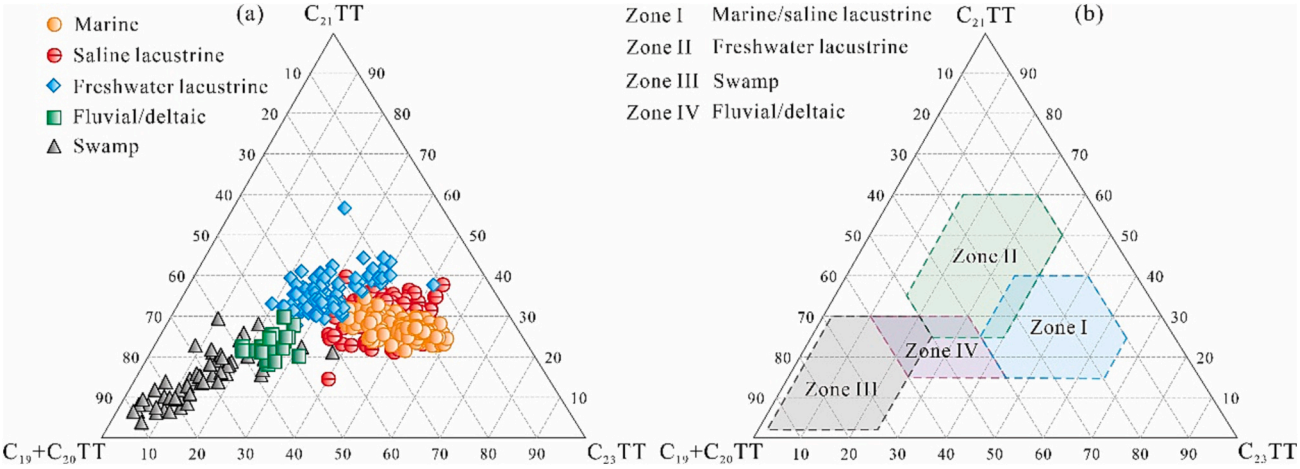

Fig. 5. Percentage of C_{19} + C_{20}TT, C_{21}TT, and C_{23}TT in marine/saline lacustrine, fluvial/deltaic, freshwater lacustrine, and swamp sediment and oil samples (a) and the reasonable separation of different depositional environments (b).

Zumberge (1987), we calculated the relative abundances of C_{19} + C_{20}TT, C_{21}TT and C_{23}TT and added them into our ternary diagram. These included 89 samples reported by Zumberge (1987) as marine (from the Cuanza, Benguela, Neuquan, North Sea, W. Canadian, Magdalans, Gulf of Suez, Oriente, Overthrust, North Slope, Nemaha, Great, Williston, Anadarko, Los Angeles, Ventura, Santa Maria, GOM, Barinas basins), 24 samples reported as deltaic/paralic (from the Vulcan, Lianos, Java Sea, Niger Delta, Indus, North Slope, Williston, GOM, Paradox, Maracaibo basins), and 31 samples reported as lacustrine (from the Congo, Benguela, Cuyo, Campos, Reconcavo, Takutu, Uinta basins), although these were not further divided into saline, brackish water and freshwater lacustrine. We further added data from 19 freshwater lacustrine samples from the Muglad Basin in Africa that were reported by Xiao et al., 2019a and 25 Triassic source rocks from the Ordos Basin (Central China) previously identified to reflect lacustrine depositional conditions by Pan et al. (2017). In addition, according to the relevant data of tricyclic terpanes reported by Tao et al. (2015), we calculated the maximum and minimum values of C_{19} + C_{20}TT%, C_{21}TT% and C_{23}TT% of 32 oil samples, including 4 Tarim marine oils, 2 Tarim saline lacustrine oils, 12 Qaidam saline lacustrine oils, 10 Ordos freshwater lacustrine oils and 4 terrigenous oils (Fig. 6). The published data show a similar distribution in the C_{19} + C_{20}TT, C_{21}TT and C_{23}TT ternary diagram (Fig. 6), demonstrating its effectiveness and world-wide applicability of our approach for the identification of depositional environments. The new method is surprisingly simple, without the need for high-end experimental instruments, complex experimental methods or special sample requirements. The identification process for C_{19}-C_{23} tricyclic terpenes is fast and facile, only requiring GC–MS analysis on a small amount of saturate hydrocarbon fractions and observation of the *m/z* 191 mass chromatograms. The method appears to be applicable not only to source rocks, but also to crude oils and a large variety of sedimentary rocks collected in the field with a thermal maturity range (at least) throughout the oil window and even for severely biodegraded samples.

5. Conclusions

We propose a relatively simple, convenient, and powerful scheme for the identification of paleo-depositional conditions of sedimentary rocks and related crude oils based on the construction of a ternary diagram of C_{19} + C_{20}, C_{21} and C_{23} tricyclic terpane distributions. Marine/saline lacustrine, freshwater lacustrine, swamp and fluvial/deltaic facies are readily distinguished in a global data set of post-Ordovician samples. We propose that the separation is mostly due to the preferential production of C_{23}TT precursors (e.g., tricyclohexaprenol) under saline conditions and the additional input of C_{19}TT and C_{20}TT precursors such as dammarenes or manool by plants and/or soil microbiota in terrestrial settings. Freshwater (lacustrine or deltaic) settings may reflect more mixed source input, but likely also reflect preferential production of as yet unknown precursors of C_{21}TT. Limited data from Ordovician and older

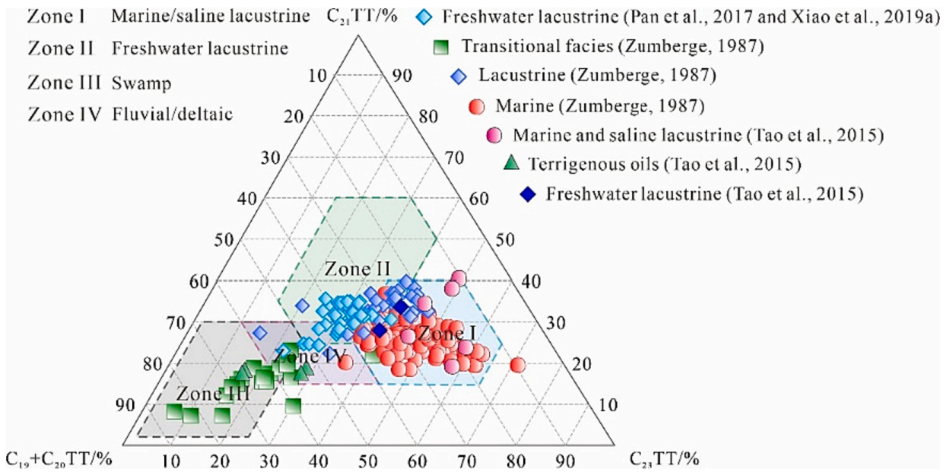

Fig. 6. Application of ternary diagram of C_{19} + C_{20} tricyclic terpanes (C_{19} + C_{20}TT), C_{21}TT and C_{23}TT.

samples indicates a likely substantial contribution of C_{19}TT and C_{20}TT from biological sources other than higher plants (e.g., microbial dammarenes) and more extensive compilations of samples predating the rise of land plants are required in the future to explore a potential calibration of short-chain TT distributions for the identification of depositional environments in Ordovician and older strata. As for all proxies, tricyclic terpane parameters should be accompanied by additional proxies and/or detailed sedimentary analyses whenever possible to improve the robustness of paleo-ecological inferences. For example, elevated gammacerane levels as reflected by enhanced gammacerane index values are often associated with salinity stratification thereby providing additional influence on saline depositional conditions, while the C_{30} sterane 24-n-propylcholesterol is typically enriched in marine samples (Moldowan et al., 1990) and tetracyclic polyprenoids are typically enriched in freshwater environments as reflected in elevated TPP ratios (Holba et al., 2003), while higher plant biomarkers such as oleanoids are typically enriched in terrestrial organic matter (Moldowan et al., 1994). Ideally, the identification of paleo-depositional conditions should thus encompass a combination of tricyclic terpane and other marker compounds and these integrated analyses should allow to further differentiate between marine and saline lacustrine depositional environments. Besides the facile application and strong predictive power, another advantage of using tricyclic terpane distributions are applicability to a wide range of thermal maturities and apparent resistance of tricyclic terpane distributions against changes induced by even severe biodegradation.

CRediT authorship contribution statement

Hong Xiao: Writing – review & editing, Writing – original draft, Visualization, Validation, Supervision, Software, Resources, Project administration, Methodology, Investigation, Funding acquisition, Formal analysis, Data curation, Conceptualization. **Meijun Li:** Supervision, Methodology, Funding acquisition, Conceptualization. **Benjamin J. Nettersheim:** Writing – original draft, Validation.

Declaration of competing interest

The authors declare that they have no known competing financial interests or personal relationships that could have appeared to influence the work reported in this paper.

Data availability

I have shared the data in a supplemental file.

Acknowledgements

The authors would like to thank the editor and three anonymous reviewers for their constructive comments and suggestions which significantly improved the quality of the manuscript. This work was supported by the National Natural Science Foundation of China (No. 42202134), Science Foundation of China University of Petroleum, Beijing (No. 2462023YJRC010) and the postdoctoral fellowship by the Central Research and Development Fund of the University of Bremen.

Appendix A. Supplementary data

Supplementary data and additional information regarding the percentage of C_{19} + C_{20}, C_{21} and C_{23} tricyclic terpanes in 485 oil and sediment samples from various formations with distinct depositional environments during the late Paleozoic to Neogene periods. Supplementary data to this article can be found online at [https://doi.org/10.1016/j.chemgeo.2024.122023].

References

Anders, D.E., Robinson, W.E., 1971. Cycloalkane constituents of the bitumen from Green River Shale. Geochim. Cosmochim. Acta 35, 661–678.
Aquino Neto, F.R., Restle, A., Connan, J., Albrecht, P., Ourisson, G., 1982. Novel tricyclic terpanes (C_{19}, C_{20}) in sediments and petroleum. Tetrahedron Lett. 23, 2027–2030.
Aquino Neto, F.R., Trendel, J.M., Restlé, A., Connan, J., Albrecht, P., 1983. Occurrence and formation of tricyclic terpanes in sediments and petroleum. In: Bjorøy, M., Albrecht, P., Cornford, C., De Groot, K., Eglinton, G., Galimov, E., Leythaeuser, D., Pelet, R., Rullkötter, J., Speers, G. (Eds.), *Advances in Organic Geochemistry* 1981. Wiley, Chichester, pp. 659–667.
Aquino Neto, F.R., Cardoso, J.N., Rodrigues, R., Trindade, L.A.F., 1986. Evolution of tricyclic alkanes in the Espirito Santo Basin, Brazil. Geochim. Cosmochim. Acta 50, 2069–2072.
Aquino Neto, F.R., Trigüis, J., Azevedo, D.A., Rodriques, R., Simoneit, B.R.T., 1992. Organic geochemistry of geographically unrelated tasmanites. Org. Geochem. 18, 791–803.
Azevedo, D.A., Aquino Neto, F.R., Simoneit, B.R.T., Pinto, A.C., 1992. Novel series of tricyclic aromatic terpanes characterized in Tasmanian tasmanite. Org. Geochem. 18, 9–16.
Bennett, B., Jiang, C., 2021. Oil-source and oil-oil correlations and the origin of the heavy oil and bitumen accumulations in Northern Alberta, Canada. Org. Geochem. 153, 104199.
Carman, R.M., Duffield, A.R., 1993. The Biosynthesis of Labdanoids. The Optical Purity of naturally Occurring Manool and Abienol. Aust. J. Chem. 46, 1105–1114.
Chen, Z., Liu, G., Wei, Y., Gao, G., Ren, J., Yang, F., Ma, W., 2017. Distribution pattern of tricyclic terpanes and its influencing factors in the Permian source rocks from Mahu Depression in the Junggar Basin. Oil Gas Geol. 38, 311–322 (in Chinese with English abstract).
Chen, G., Wang, D., Yang, F., Tang, Y., Zou, X., Ma, W., Li, M., 2022. Organic geochemistry and controlling factors of alkaline source rocks within sequence stratigraphic framework in the Fengcheng Formation, Mahu Sag, Junggar Basin, NW China. Energy Explor. Exploit. 40, 1057–1077.
Cheng, X., Hou, D., Xu, C., Wang, F., 2016. Biodegradation of tricyclic terpanes in crude oils from the Bohai Bay Basin. Org. Geochem. 101, 11–21.
Cheng, X., Hou, D., Zhou, X., Liu, J., Diao, H., Jiang, Y., Yu, Z., 2020. Organic geochemistry and kinetics for natural gas generation from mudstone and coal in the Xihu Sag, East China Sea Shelf Basin, China. Mar. Pet. Geol. 118, 104405.
De Grande, S.M.B., Aquino Neto, F.R., Mello, M.R., 1993. Extended tricyclic terpanes in sediments and petroleums. Org. Geochem. 20, 1039–1047.
Ekweozor, C.M., Strausz, O.P., 1982. 18,19-Bisnor-13βH, 14-αh-cheilanthane: a novel degraded tricyclic sesterterpenoid-type hydrocarbon from the athabasca oil sands. Tetrahedron Lett. 23, 2711–2714.
Farrimond, P., Bevan, J.C., Bishop, A.N., 1999. Tricyclic terpane maturity parameters: response to heating by an igneous intrusion. Org. Geochem. 30, 1011–1019.
Fu, J., Zhang, Z., Chen, C., Wang, T.G., Li, M., Ali, S., Lu, X., Dai, J., 2019. Geochemistry and origins of petroleum in the Neogene reservoirs of the Baiyun Sag, Pearl River Mouth Basin. Mar. Pet. Geol. 107, 127–141.
Gan, H., Wang, H., Shi, Y., Ma, Q., Liu, E., Yan, D., Pan, Z., 2020. Geochemical characteristics and genetic origin of crude oil in the Fushan sag, Beibuwan Basin, South China Sea. Mar. Pet. Geol. 112, 104114.
Genik, G.J., 1993. Petroleum geology of Cretaceous-Tertiary rift basins in Niger, Chad, and Central African Republic. AAPG Bull. 77, 1405–1434.
Graas, G.W.V., 1990. Biomarker maturity parameters for high maturities: Calibration of the working range up to the oil/condensate threshold. Org. Geochem. 16, 1025–1032.
Greenwood, P.F., Arouri, K.R., George, S.C., 2000. Tricyclic terpenoid composition of tasmanites kerogen as determined by pyrolysis GC-MS. Geochim. Cosmochim. Acta 64, 1249–1263.
Hanson, A.D., Zhang, S.C., Moldowan, J.M., Liang, D.G., Zhang, B.M., 2000. Molecular organic geochemistry of the Tarim Basin, Northwest China. AAPG Bull. 84, 1109–1128.
Head, I.M., Jones, D.M., Larter, S.R., 2003. Biological activity in the deep subsurface and the origin of heavy oil. Nature 426, 344–352.
Holba, A.G., Dzou, L.I., Wood, G.D., Ellis, L., Adam, P., Schaeffer, P., Albrecht, P., Greene, T., Hughes, W.B., 2003. Application of tetracyclic polyprenoids as indicators of input from fresh-brackish water environments. Org. Geochem. 34, 441–469.
Holzer, G., Oró, J., Tornabene, T.G., 1979. Gas chromatographic—mass spectrometric analysis of neutral lipids from methanogenic and thermoacidophilic bacteria. J. Chromatogr. A 186, 795–809.
Hu, L., Fuhrmann, A., Poelchau, H.S., Horsfield, B., Zhang, Z., Wu, T., Chen, Y., Li, J., 2005. Numerical simulation of petroleum generation and migration in the Qingshui sag, western depression of the Liaohe basin, Northeast China. AAPG Bull. 89, 1629–1649.
Huang, B., Xiao, X., Cai, D., Wilkins, R.W.T., Liu, M., 2011. Oil families and their source rocks in the Weixinan Sub-basin, Beibuwan Basin, South China Sea. Org. Geochem. 42, 134–145.
Khan, H., Zaman, A., Chetty, G.L., Gupta, A.S., Dev, S., 1971. Cheilanthatriol - a new fundamental type in sesterterpenes. Tetrahedron Lett. 12, 4443–4446.
Li, S., Pang, X., Li, M., Jin, Z., 2003. Geochemistry of petroleum systems in the Niuzhuang South Slope of Bohai Bay Basin—part 1: source rock characterization. Org. Geochem. 34, 389–412.
Luo, K., Lu, J., Chen, L., 2005. Lead distribution in Permo-Carboniferous coal from the North China Plate, China. Environ. Geochem. Hlth. 27, 31–37.
McHargue, T.R., Heidrick, T.L., Livingston, J.E., 1992. Tectonostratigraphic development of the Interior Sudan rifts, Central Africa. Tectonophysics 213, 187–202.

Mello, M.R., Gaglianone, P.C., Brassell, S.C., Maxwell, J.R., 1988. Geochemical and biological marker assessment of depositional environments using Brazilian offshore oils. Mar. Pet. Geol. 5, 205–223.
Meunier-Christmann, C., Albrecht, P., Brassell, S.C., Ten Haven, H.L., Van Der Linden, B., Rullkötter, J., Trendel, J.M., 1991. Occurrence of dammar-13(17)-enes in sediments: Indications for a yet unrecognized microbial constituent? Geochim. Cosmochim. Acta 55 (11), 3475–3483.
Ming, C., Hou, D., Zhao, X., Song, J., Deng, J., Wu, S., Li, J., 2015. The Geochemistry Records of Paleoenvironment and Sea-Level Relative Movement of Middle Permian Zhesi Formation in Eastern Inner Mongolia. Acta Geol. Sin. 89, 1484–1494 (in Chinese with English abstract).
Moldowan, J.M., Seifert, W.K., Gallegos, E.J., 1983. Identification of an extended series of tricyclic terpanes in petroleum. Geochim. Cosmochim. Acta 47, 1531–1534.
Moldowan, J.M., Fago, F.J., Lee, C.Y., Jacobson, S.R., Watt, D.S., Slougui, N.E., Jeganathan, A., Young, D.C., 1990. Sedimentary 24-n-Propylcholestanes, Molecular Fossils Diagnostic of Marine Algae. Science 247, 309–312.
Moldowan, J.M., Dahl, J., Huizinga, B.J., Fago, F.J., Hickey, L.J., Peakman, T.M., Taylor, D.W., 1994. The molecular fossil record of oleanane and its relation to angiosperms. Science 265, 768–771.
Ourisson, G., Albrecht, P., Rohmer, M., 1982. Predictive microbial biochemistry—from molecular fossils to procaryotic membranes. Trends Biochem. Sci. 7, 236–239.
Palacas, J.G., Monopolis, D., Nicolaou, C.A., Anders, D.E., 1986. Geochemical correlation of surface and subsurface oils, western Greece. Org. Geochem. 10, 417–423.
Pan, S., Horsfield, B., Zou, C., Yang, Z., Gao, D., 2017. Statistical analysis as a tool for assisting geochemical interpretation of the Upper Triassic Yanchang Formation, Ordos Basin, Central China. Int. J. Coal Geol. 173, 51–64.
Peters, K.E., Moldowan, J.M., 1993. The Biomarker Guide: Interpreting Molecular Fossils in Petroleum and Ancient Sediments. Prentice Hall, Englewood Cliffs, New Jersey.
Peters, K.E., Walters, C.C., Moldowan, J.M., 2005. The Biomarker Guide: Biomarkers and Isotopes in Petroleum Exploration and Earth history. In: Seconded, vol. 2. Cambridge University Press, Cambridge.
Philp, P., Symcox, C., Wood, M., Nguyen, T., Wang, H., Kim, D., 2021. Possible explanations for the predominance of tricyclic terpanes over pentacyclic terpanes in oils and rock extracts. Org. Geochem. 155, 104220.
Powell, T.G., 1986. Petroleum geochemistry and depositional setting of lacustrine source rocks. Mar. Pet. Geol. 3, 200–219.
Preston, J.C., Edwards, D.S., 2000. The petroleum geochemistry of oils and source rocks from the northern Bonaparte Basin, offshore northern Australia. APPEA J. 40, 257–282.
Reed, W.E., 1977. Molecular compositions of weathered petroleum and comparison with its possible source. Geochim. Cosmochim. Acta 41, 237–247.
Revill, A.T., Volkman, J.K., O'Leary, T., Summons, R.E., Boreham, C.J., Banks, M.R., Denwer, K., 1994. Hydrocarbon biomarkers, thermal maturity, and depositional setting of tasmanite oil shales from Tasmania, Australia. Geochim. Cosmochim. Acta 58, 3803–3822.
Schwark, L., Frimmel, A., 2004. Chemostratigraphy of the Posidonia Black Shale, SW-Germany: II. Assessment of extent and persistence of photic-zone anoxia using aryl isoprenoid distributions. Chem. Geol. 206, 231–248.
Seifert, W.K., Moldowan, J.M., 1978. Applications of steranes, terpanes and monoaromatics to the maturation, migration and source of crude oils. Geochim. Cosmochim. Acta 42, 77–95.
Simoneit, B.R.T., Leif, R.N., Aquino Neto, F.R., Azevedo, D.A., Pinto, A.C., Albrecht, P., 1990. On the presence of tricyclic terpane hydrocarbons in Permian tasmanite algae. Naturwissenschaften 77, 380–383.
Simoneit, B.R.T., Schoell, M., Dias, R.F., Aquino Neto, F.R., 1993. Unusual carbon isotope compositions of biomarker hydrocarbons in a Permian tasmanite. Geochim. Cosmochim. Acta 57, 4205–4211.
Stojanović, K., Jovančićević B, Pevneva, G.S., Golovko, J.A., Golovko, A.K., Pfendt, P., 2001. Maturity assessment of oils from the Sakhalin oil fields in Russia: phenanthrene content as a tool. Org. Geochem. 32, 721–731.
Sun, Y., Xu, S., Lu, H., Cuai, P., 2003. Source facies of the Paleozoic petroleum systems in the Tabei uplift, Tarim Basin, NW China: implications from aryl isoprenoids in crude oils. Org. Geochem. 34, 629–634.
Tao, S., Wang, C., Du, J., Liu, L., Chen, Z., 2015. Geochemical application of tricyclic and tetracyclic terpanes biomarkers in crude oils of NW China. Mar. Pet. Geol. 67, 460–467.
Volk, H., George, S.C., Middleton, H., Schofield, S., 2005. Geochemical comparison of fluid inclusion and present-day oil accumulations in the Papuan Foreland – evidence for previously unrecognised petroleum source rocks. Org. Geochem. 36, 29–51.
Wang, C., Du, J., Wang, W., Wu, B., Zhou, X., 2012. Distribution and isomerization of terpanes in pyrolyzates of lignite at high pressures and temperatures. J. Pet. Geol. 35, 377–387.
Wang, Y., Cao, J., Li, X., Zhang, J., Wang, Y., 2019. Cretaceous and Paleogene saline lacustrine source rocks discovered in the southern Junggar Basin, NW China. J. Asian Earth Sci. 185, 104019.
Wang, A., Li, C., Li, L., Pu, R., Yang, Z., Zhu, N., Huo, K., 2023. C_{20}-C_{21}-C_{23} tricyclic terpanes abundance patterns: Origin and application to depositional environment identification. Front. Earth Sci. 11, 1128692.
Xiao, H., Wang, T.G., Li, M., Fu, J., Tang, Y., Shi, S., Yang, Z., Lu, X., 2018. Occurrence and distribution of unusual tri- and tetracyclic terpanes and their geochemical significance in some Paleogene oils from China. Energy Fuel 32, 7393–7403.
Xiao, H., Li, M., Liu, J., Mao, F., Cheng, D., Yang, Z., 2019a. Oil-oil and oil-source rock correlations in the Muglad Basin, Sudan and South Sudan: New insights from molecular markers analyses. Mar. Pet. Geol. 103, 351–365.
Xiao, H., Li, M., Yang, Z., Zhu, Z., 2019b. Distribution patterns and geochemical implications of C_{19}–C_{23} tricyclic terpanes in source rocks and crude oils occurring in various depositional environments. Acta Geochim. 49, 161–170 (in Chinese with English abstract).
Xiao, H., Wang, T.G., Li, M., Lai, H., Liu, J., Mao, F., Tang, Y., 2019c. Geochemical characteristics of cretaceous Yogou Formation source rocks and oil-source correlation within a sequence stratigraphic framework in the Termit Basin, Niger. J. Pet. Sci. Eng. 172, 360–372.
Xiao, H., Wang, T.G., Li, M., Cheng, D., Yang, Z., 2021a. Organic geochemical heterogeneity of the cretaceous Abu Gabra Formation and reassessment of oil sources in the Sufyan Sub-basin, Sudan. Org. Geochem. 162, 104301.
Xiao, H., Wang, T.G., Li, M., You, B., Zhu, Z., 2021b. Extended series of tricyclic terpanes in the Mesoproterozoic sediments. Org. Geochem. 156, 104245.
Yang, F., Wang, T., Li, M., 2016. Oil filling history of the Mesozoic oil reservoir in the Tabei Uplift of Tarim Basin, NW China. J. Pet. Sci. Eng. 142, 129–140.
Yang, Z., Li, M., Cheng, D., Xiao, H., Lai, H., Chen, Q., 2019. Geochemistry and possible origins of biodegraded oils in the cretaceous reservoir of the Muglad Basin and their application in hydrocarbon exploration. J. Pet. Sci. Eng. 173, 889–898.
You, B., Ni, Z., Zeng, J., Luo, Q., Xiao, H., Song, G., Wang, Y., 2020. Oil-charging history constrained by biomarkers of petroleum inclusions in the Dongying Depression, China. Mar. Pet. Geol. 122, 104657.
You, B., Ni, Z., Chen, J., Wang, G., Xiao, H., Wang, Y., Song, G., 2021. A distinct oil group in the Dongying Depression, Bohai Bay Basin, China: New insights from norcholestane and triaromatic steroid analyses. Org. Geochem. 162, 104316.
Zeng, B., Li, M., Wang, N., Shi, Y., Wang, F., Wang, X., 2022. Geochemistry and heterogeneous accumulation of organic matter in lacustrine basins: A case study of the Eocene Liushagang Formation in the Fushan Depression, South China Sea. Pet. Sci. 19, 2533–2548.
Zhang, S., Huang, H., 2005. Geochemistry of Palaeozoic marine petroleum from the Tarim Basin, NW China: part 1. Oil family classification. Org. Geochem. 36, 1204–1214.
Zhang, C., Zhang, Y., Cai, C., 2011. Aromatic isoprenoids from the 25–65Ma saline lacustrine formations in the western Qaidam Basin, NW China. Org. Geochem. 42, 851–855.
Zhang, B., He, Y., Chen, Y., Meng, Q., Huang, J., Yuan, L., 2018. Formation of mechanism of saline lacustrine source rocks in western Qaidam Basin. Acta Petrol. Sin. 39, 674–685 (in Chinese with English abstract).
Zhou, F., Zhang, Y., Liu, Z., Sui, G., Li, G., Wang, C., Cui, S., Zhang, Y., Wang, J., Zhu, J., 2016. Geochemical characteristics and origin of natural gas in the Dongping–Niudong areas, Qaidam Basin, China. J. Nat. Gas Geosci. 1, 489–499.
Zhu, Y., Weng, H., Su, A., Liang, D., Peng, D., 2005. Geochemical characteristics of Tertiary saline lacustrine oils in the Western Qaidam Basin, Northwest China. Appl. Geochem. 20, 1875–1889.
Zumberge, J.E., 1983. Tricyclic diterpane distributions in the correlation of Paleozoic crude oils from the Williston Basin. In: Bjorøy, M., Albrecht, P., Cornford, C., De Groot, K., Eglinton, G., Galimov, E., Leythaeuser, D., Pelet, R., Rullkötter, J., Speers, G. (Eds.), Advances in Organic Geochemistry, 1981. Wiley, Chichester, pp. 738–745.
Zumberge, J.E., 1987. Prediction of source rock characteristics based on terpane biomarkers in crude oils: A multivariate statistical approach. Geochim. Cosmochim. Acta 51, 1625–1637.